Hit or Miss: Sensor Design via Scaled Collision Theory

Wenjun Zhang, S.M.ASCE[1]; Sheyda Nazarian, S.M.ASCE[2]; Ming Wang, M.ASCE[3]; and Steve W. Cranford, M.ASCE[4]

Abstract: The working characteristics of targeted surface sensing systems—such as fluid velocity and concentration limits—have mostly been explored through experimental trials. Here we develop a novel scaled collision theory to facilitate the experimental screening process in determining the optimal system parameters specific to sensing discrete molecular or particulate targets with low concentration in a bulk fluid system, such as biomarkers, pollutants, or explosives. A simple fluid sensor system was developed and subjected to steady-state Couette flow to explore key parameters. Validated by 177 particle-based coarse-grain simulations, this theory indicates that the chance of successful pairing events between molecular markers and its corresponding targets—or hits—is determined by their concentrations, binding affinity or energy, and more importantly the flow velocity. Scaled collision theory reveals great potential to be used as a system design tool for a wide spectrum of sensing applications, ranging from water and air quality monitoring to biomedical detection and disease diagnostics. **DOI: 10.1061/(ASCE)EM.1943-7889.0001487.** © *2018 American Society of Civil Engineers.*

Author keywords: Sensor interface; Fluid dynamics; Collision theory; Molecular simulation; Couette flow.

Introduction

Targeted surface sensors are analytical devices that are designed to indicate the presence and quantity of a certain component in a bulk fluid. Typically, active sites or catalysts on a sensor have unique reaction proclivities with a target. Examples include platforms for explosive detection (Engel et al. 2010; Peters et al. 2015), DNA-decorated carbon nanotubes for breath and air monitoring (Zhang et al. 2016), water pollutant exposure (Lefevre et al. 2012), heavy metal measurement (Jung et al. 2011), or bioassays (Dixit and Kaushik 2012). Many such systems are currently under development, including combinatorial sensors capable of detecting multiple particulate types (Cao et al. 2015; Dawoud et al. 2007; Ko et al. 2008; Lee et al. 2015). While sensors may be highly reactive to their intended targets, their success is highly dependent on their active environmental conditions, including target concentration, pressure, and temperature. One key criterion is fluid behavior, which can be potentially controlled via microfluidics (Mark et al. 2010). With throughput processing, enhanced control of flow conditions, and increased sensitivity of detection, microfluidic techniques have been widely applied to a variety of environmental aspects such as monitoring of water, air, and food quality; and detection of microorganisms, biofilms, environmental pollutants, and toxins (Cate et al. 2015; Lisowski and Zarzycki 2013; Marle and Greenway 2005; Meredith et al. 2016; Zhao and Dong 2013). Integrated with sensor development, microfluidic systems provide great advantages in a broad spectrum of molecular screening applications, such as environmental engineering, biomedical detection, point-of-care diagnostics, and explosive detection (Chu et al. 2015; Gowers et al. 2015; Kumar et al. 2013; Yeo et al. 2011; Zhou et al. 2015) [Fig. 1(a)]. For the continuing innovation of such sensing technologies, thorough theoretical knowledge of active surface–fluid interaction is critical for predictive design.

The basis of such sensors lies in the continuous sampling of a bulk fluid as it crosses an activated surface [Fig. 1(b)]. A target molecule must contact (or be in close proximity to) an interaction point for any detection to be recorded (depending on the reaction mechanism)—a kind of hit-or-miss selectivity condition [Fig. 1(c)]. However, in designing such microfluidic systems, parameters like concentrations, especially flow velocity, are typically chosen according to the literature or experimental trial and error.

Here, we develop a predictive theory to guide the selection and optimization of the parameters with respect of different sensing applications. The approach is based on collision theory coupled with simple fluid flow and interaction parameters. We are effectively looking for a detection rate, akin to kinetic chemical reaction rates, described by the classical Arrhenius relation or collision theory, or bond dissociation rates, encapsulated by Bell's model. Chemical kinetics can be loosely mapped to fluid dynamics by means of similar interaction events. These interactions are modeled directly via a molecular dynamics (MD) approach, with explicit fluid, particles, and interaction sites defined, and the time history of the flow providing the statistical sampling space. Other approaches could provide the same results, including analytical statistical solutions [e.g., Markov chain model (Kapral 2008)], continuum-based (i.e., stochastic fluid dynamics) (Gompper et al. 2009), or Monte Carlo approaches (Bialik 2011).

In each case, a chemical event occurs if the molecular energy is sufficient to overcome the defined activation energy across a number of stochastic trials (based on, for example, molecular density for collision theory, or molecular vibration in the case of bond breaking), and the current energetic conditions (e.g., temperature). Typically, activation energy and other constants are determined empirically, representing reaction-specific parameters difficult to predict from ab initio threshold energies. However, such models

[1]Laboratory for Nanotechnology in Civil Engineering, Sensor Technologies Lab, College of Engineering, Northeastern Univ., Boston, MA 02115.

[2]Laboratory for Nanotechnology in Civil Engineering, Sensor Technologies Lab, College of Engineering, Northeastern Univ., Boston, MA 02115.

[3]Sensor Technologies Lab, Dept. of Civil and Environmental Engineering, Northeastern Univ., Boston, MA 02115.

[4]Laboratory for Nanotechnology in Civil Engineering, Dept. of Civil and Environmental Engineering, Northeastern Univ., Boston, MA 02115 (corresponding author). Email: s.cranford@northeastern.edu

Note. This manuscript was submitted on November 8, 2017; approved on January 31, 2018; published online on June 20, 2018. Discussion period open until November 20, 2018; separate discussions must be submitted for individual papers. This paper is part of the ***Journal of Engineering Mechanics***, © ASCE, ISSN 0733-9399.

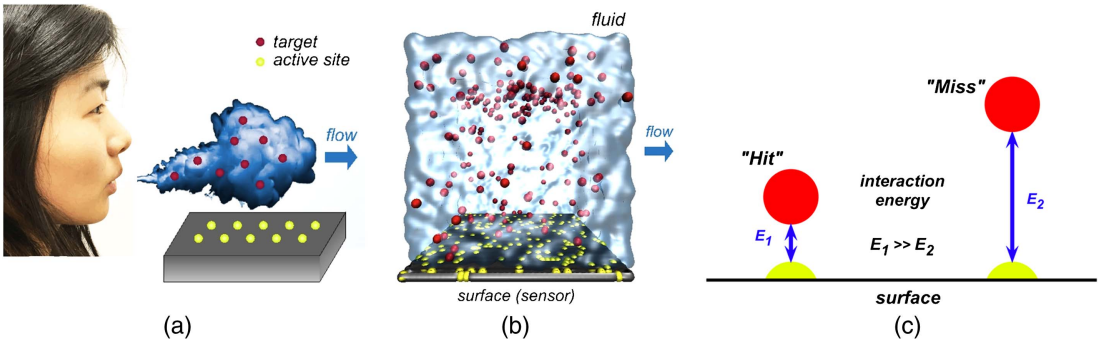

Fig. 1. Scaled collision theory application and model system: (a) example application of sensor array for breath analysis; molecular biomarkers in breath detected by active sites on an activated material platform (image by Steve W. Cranford); (b) ideal system to be modeled via MD particle-based simulation, consisting of bulk fluid with random distribution of target markers flowing over a fixed surface (sensor) with a random distribution of active sites; and (c) definition of particle hit or miss based on interaction energy.

have been highly successful in phenomenologically describing reaction rates. To explore the veracity of this collision theory approach, we devise a simple fluid–surface system to systematically explore the effects of fluid and surface properties.

Model System

The model system consisted of a two-phase fluid atop a planar two-dimensional surface lattice. The fluid particles were defined as either bulk or randomly distributed target particles with a set concentration, c_1. The fixed surface particles were also defined as either bulk or randomly distributed anchor particles with a set concentration, c_2. Interactions between all particles replicate ideal fluid behavior (see the "Methods" section). The fluid was then subject to steady-state Couette flow, and the number of target–anchor pairings was determined over time (e.g., successful sensing rate).

Couette flow is typically described by the laminar flow of a viscous fluid in the space between two parallel plates. Our system assumed such an arrangement for the inlet of a potential sensor. It behooves us to note that while the computational method relies on a molecular dynamics framework, the simulations themselves were effectively scale-free (i.e., collisions could be assumed at the mesoscale). From a nanoscale perspective, the assumption of Newtonian flow is a computational convenience, representing the simplest flow case, by achieving predictable flow and velocity at the fluid–surface interface. Planar Couette flow with no body forces is described by the incompressible Navier-Stokes equations (Schlichting 1955), which provide a one-dimensional approximation to the geometry presented. The x-component of the velocity profile, $u(y,t)$, is given by

$$\rho\frac{\partial u}{\partial t} = \mu\frac{\partial^2 u}{\partial y^2} \tag{1a}$$

For constant flow, $\partial u/\partial t = 0$, such that $u(y)$ is linear, and a function of the viscosity, μ, and the prescribed boundary conditions. In general, Couette flow assumes no slip at the boundaries [e.g., velocity of the fluid relative to the wall is zero at the solid–fluid interface, or $u(y) = 0$]. Here, due to the prescribed Lennard-Jones (LJ) potential, slipping is allowed. Once the flow profile fully develops, the velocity at the interface is approximately constant (and linearly dependent on the prescribed velocity at the upper boundary), or

$$u(y) = Ay + B \tag{1b}$$

where A and B = function of viscosity, μ, and related to the prescribed LJ interaction parameter. The upper fluid is subject to a driving velocity, developing the necessary velocity profile (Fig. 2 and the "Methods" section).

Scaled Collision Theory

To facilitate sensor parameter selection particularly for detection through binding reactions, we developed a nonconventional collision theory applicable to microscale fluid flow called scaled collision theory (SCT). Collision theory, proposed independently by Trautz (1916) and Lewis (1918), quantitatively explains how chemical reactions occur and why reaction rates vary for different reactions (IUPAC 1997). For molecular kinetics, it predicts a rate of chemical reaction as follows:

$$b(T) = \beta Z \exp\left(\frac{-E_a}{bT}\right) \tag{2}$$

where β = steric factor; Z = collision frequency; E_a = activation energy for the reaction; and bT = thermal energy (b being Boltzmann's constant, and T the temperature). Collision theory states that when suitable particles of the reactant hit each other, a certain percentage results in chemical reaction if they have enough energy to exceed the activation energy at the moment of impact. Increasing the concentration (more collisions) or raising the temperature (more collisions and higher energy) thus increases the rate of reaction. We wish to convert the reaction rate to a sensing rate, k, where the sensing rate is the number of detected molecular targets per second per area of a sensor surface.

Applied to a general sensing system, we revise the key parameters using Eq. (2) as a basis. Our desired rate is the number of successful target–anchor pairings, or hits, per second per area. In this case, we have a concentration of targets in the fluid (c_1, in m^{-3}) and a concentration of anchors on the surface (c_2, in m^{-2}). We also have a volumetric flow of the fluid over the surface, v (m^3/s). Thus, our prefactor representing the potential pair frequency is simply $Z = c_1 c_2 v$, which results in the desired units of $\mathrm{m}^{-2}\,\mathrm{s}^{-1}$. For the term within the exponential in Eq. (2), we recognize that (1) the activation energy must be overcome to result in a successful reaction, and (2) increasing the thermal energy increases the energy available, and thus increases the likelihood of reaction. Here the circumstance is somewhat reversed—the set interaction energy,

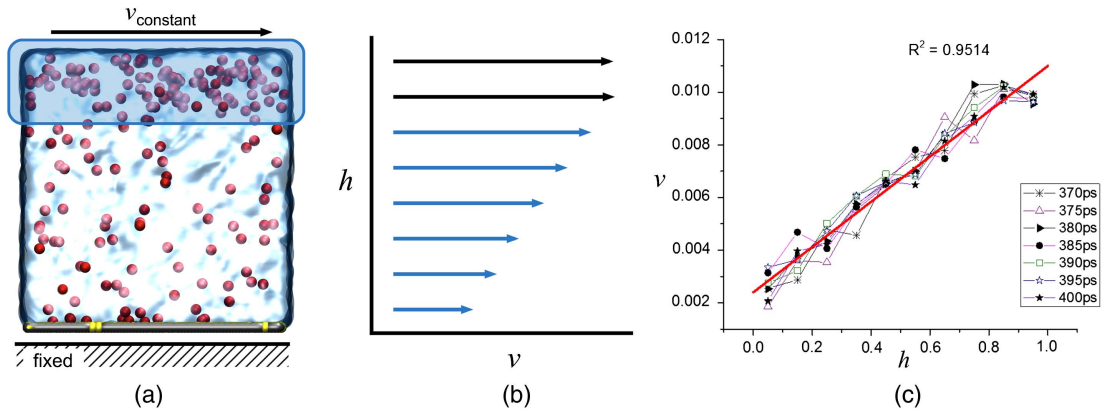

Fig. 2. Model flow conditions: (a) model boundary conditions where the top one-fifth of fluid is subject to constant velocity, surface–substrate is fixed, and the system is allowed to equilibrate; (b) ideal developed Couette flow (linear increase) with an applied constant velocity (top two arrows) at the top layer of the fluid; and (c) velocity profile (velocity versus height) at the end of equilibration, which depicts near-constant linear profile over range of time steps, with finite velocity at the fluid–surface interface.

ε, between target and anchor promotes hits, while the thermal or kinetic energy must be overcome to remove the target from the bulk flow. We further substitute the kinetic energy of the flow in place of the temperature term (equivalent at the molecular scale). This interpretation results in

$$k(v) = \beta c_1 c_2 v \cdot \exp\left(-\alpha \frac{v^2}{\varepsilon}\right) \tag{3}$$

We maintain a unitless constant β to account for unsuccessful matchings and the parameter α (units of mass) to account for fluid and flow characteristics (e.g., fluid mass and turbulence). In order to validate this SCT formula [Eq. (3)], we systematically explore the target–anchor concentrations, adhesion energy, and flow velocities and the effect on sensor hits.

Methods

We implemented a coarse-grained MD technique to model fluid flow by representing fluid as a system of spherical particles (Padding and Briels 2002). All simulations were performed using the open-source MD code LAMMPS (Plimpton 1995). The fluid molecules interact with themselves and the surface particles through the classical LJ 12:6 potential. Interaction parameters are given in the Supplemental Data. The surface, which is fixed, was modeled by a regular triangular lattice, with anchor particles randomly distributed. The fluid was initially arranged in a crystalline lattice and allowed to randomly distribute via high-temperature diffusion until order was lost. Target particles were then randomly distributed. Periodic conditions were implemented; the upper portion of the fluid was held fixed, while the surface defined the lower system boundary. To develop Couette flow, the top one-fifth (20% by height) of the fluid system was selected at a prescribed set velocity, v_0, in the flow direction. To ensure the simulations achieved steady-state efficiently, the remaining free fluid was given an initial velocity of $0.8v_0$ and allowed to evolve over time until velocities across the height remained near constant (see Supplemental Data), requiring approximately 200,000 integration steps. The system was run at a steady state for an additional 200,000 integration steps to collect fluid–surface interaction energetics. Hits were assessed by tracking the total interaction energy between target and anchor particles. It was accomplished by first subtracting the energy of anchor–anchor interaction from the total energy of anchor particles, and then dividing by one target–anchor pair's interaction energy. The average total energy was then normalized by the prescribed interaction strength of the LJ potential (see Supplemental Data).

Results and Discussion

To explore the validity of Eq. (3), we assess the number of surface hits as a function of (1) target–anchor concentrations (c_1, c_2), (2) adhesion energy (ε), and (3) flow velocity (v) via a suite of simulations.

Target–Anchor Concentrations

In terms of concentration effect, Eq. (3) predicts a linear correlation between the hits and either concentration, for example, the number of hits would double when the concentration of either the targets in the detection fluid or the anchor on the surface doubles. From a statistical standpoint, the probability of any two pair interactions between the fluid and surface corresponding to a target or anchor increases with both c_1 and c_2. We examined this assumption through applying two series of target–anchor concentrations at two arbitrary adhesion energies (5 and 10 kcal/mol) with a constant velocity of 1 nm/ps. [Fig. 3(a)]. At these two different adhesion energy conditions, doubling the target's concentrations or the anchor's concentrations both doubled the number of hits, as predicted. The variance of hit values for each system was approximately 10% of the mean, supporting the reliability of the simulation results. In effect, the $c_1 c_2$ term in Eq. (3) could easily be reduced to a single parameter, $\bar{c}$, reflective of the concentration product (or the compound probability of a matching target–anchor pair), as depicted in Fig. 3(b).

Adhesion Energy

Here, adhesion energy was reflective of the interaction energy between the target and anchor site, which in general can represent the sensitivity of the sensor's active component. One would anticipate that increasing the energy would increase the successful hit rate. Following the traditional approach to determine temperature dependence in collision theory, taking the logarithm of Eq. (3) results in

J. Eng. Mech., 2018, 144(9): 04018076

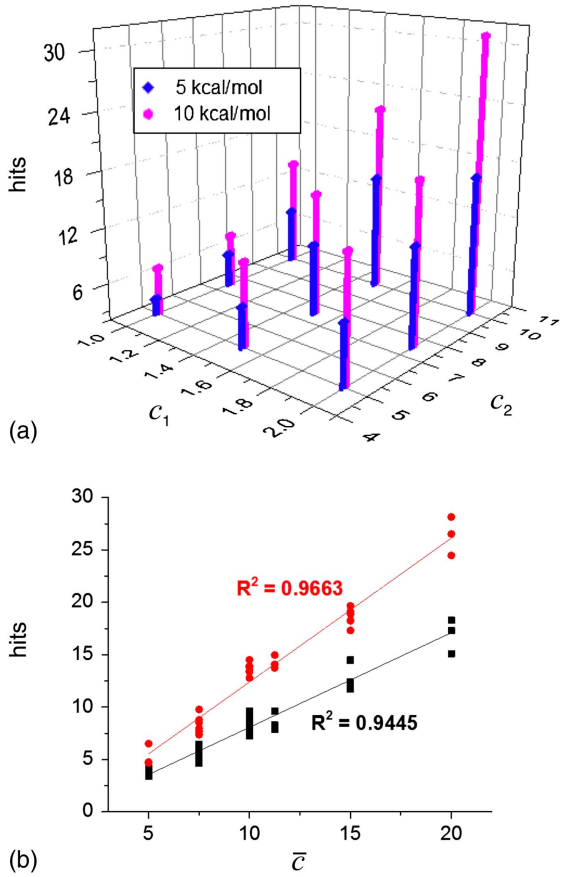

Fig. 3. Concentration effect: (a) variation of hit rate (hits) as a function of target concentration (c_1) in fluid and anchor concentration (c_2) on surface, demonstrating linear proportionality as predicted by Eq. (3) for two adhesion values ($\varepsilon = 5$ and 10 kcal/mol); and (b) concentrations reduced to single compound probability of a matching target–anchor pair, $\bar{c}$, where $\bar{c} = c_1 c_2$, also indicating linear proportionality.

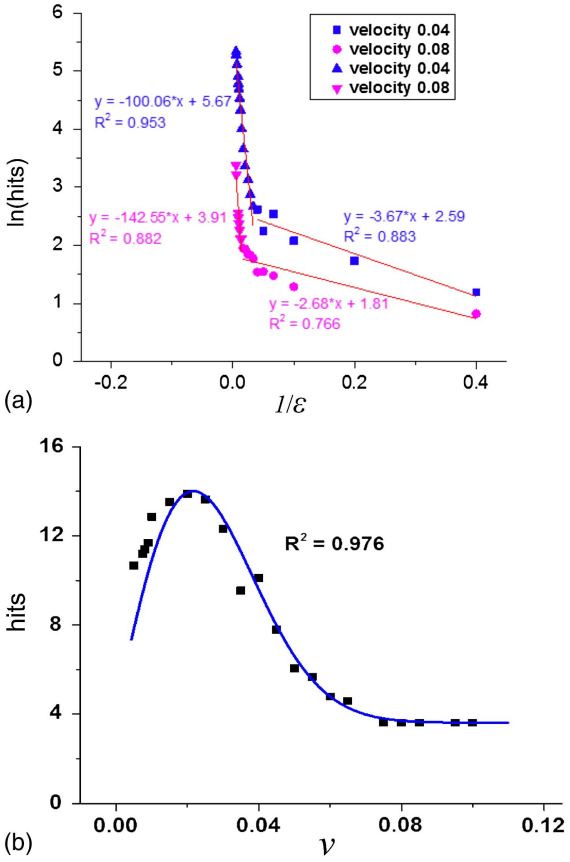

Fig. 4. Nonlinear effects: (a) variation of logarithm of hit rate [ln(hits)] as a function of the inverse of adhesion energy ($1/\varepsilon$), demonstrating two linear regimes for two trial velocities (4 and 8 nm/ps). As the adhesion energy increases, the hit rate increases, as predicted by Eq. (4). The rate of increase is heightened approximately when ε exceeds the kinetic energy of the target molecules; and (b) variation in hit rate (hits) with variation in velocity, indicating close fit with Eq. (3) and indicating optimal flow velocity.

$$\ln(k) = \ln(\beta c_1 c_2 v) - \alpha v^2 \left(\frac{1}{\varepsilon}\right) \tag{4}$$

which, for set concentrations and constant velocity, results in a linear relation with ε^{-1}. We note that as $\varepsilon \to 0$, $\varepsilon^{-1} \to \infty$, which results in an exponentially decreasing hit rate. Even at zero interaction energy, there is a nominal change that a target is in the proximity of an anchor site. Likewise, $\varepsilon \to \infty$, $\varepsilon^{-1} \to 0$, setting the upper bound for successful hits (i.e., $k_{\max} = \beta c_1 c_2 v$). More interesting, a two-stage linear correlation was observed between $\ln(k)$ and ε^{-1} for velocity of both 0.004 and 0.008 nm/fs (0.04 *and* 0.08 Å/fs) [Fig. 4(a)], indicating a phenomenological regime change dependent on ε. As adhesion energy between target and anchor increases, the attraction between these two types of molecules becomes stronger, which affects the flow characteristics and thus a higher value of α was observed when the adhesion energy was larger than approximately 50–100 kcal/mol (depending on the flow velocity). This is on the order of the average kinetic energy of each particle—when the surface adhesion becomes sufficient to halt the moving particle, the rate of hits increases at a higher rate.

Velocity

To probe the influence of velocity, we ran a suite of simulations with flow speeds ranging from 0 to 100 nm/ps. There was a clear peak and decline in hits with respect to velocity [Fig. 4(b)]. The investigation on the effect of velocity revealed a 97.6% fitting between simulated results and a linear-exponential equation as expected from Eq. (4). At low velocity, a linear relationship dominated, whereas the negative power function embedded exponential relationship began to overshadow the linear one along the increase of velocity. Simply put, when the liquid flows faster, the chance of hits increases; however, above a certain velocity value the liquid moves too quickly to have opportunities to interact with the surface. This value was called the optimal liquid flow velocity for sensing purposes. A baseline value, 3.62 hits, was observed regardless of the applied velocity values to the system, which is believed to be a result of particles' random Brownian motion in the fluid (Wiener 1921). Our simulation methodology fails to depict the decrease in hits due to decreasing velocity because the initial fluid arrangement was over the active surface upon model initialization (theoretically, hit rate decreases to zero as flow approaches zero because there would be no fluid to sample).

Conclusion

The findings here confirm the accuracy and reliability of our novel scaled collision theory, providing detailed insights into the effects of

concentration, adhesion energy, and velocity terms. It can be readily adapted to surface sensing technologies for biomedical application, environmental monitoring, and even explosive detection—any circumstance wherein a nominal amount of material must be detected from a bulk fluid. The theory, illustrated by $k(v) = \beta c_1 c_2 v \cdot \exp[-\alpha(v^2/\varepsilon)]$ reveals that pairing a molecular target with an active site on a surface depends linearly on concentration, exponentially on adhesion energy, and linear-exponentially on velocity. We demonstrated that in terms of sensor performance, faster is better, but not too fast.

This paper presented scaled collision theory, a novel nonconventional collision theory for microfluidic sensor design purpose. It can facilitate the experimental screening process in determining the optimal system parameters specific for particular molecular targets. Like most MD-based simulations, the velocities were large (exceeding 100 m/s), while the accessible timescale was relatively small (less than a nanosecond). However, unlike atomistic simulation, the model parameters here did not represent particular material parameters, and the LJ interactions can be considered general. While the velocities used in the model were experimentally inaccessible, the general proposed theory is scale-free. As such, this phenomenological theory indicates that the chance of successful pairing events between molecular targets and its corresponding pointers, hits, can be quantitatively predicted by their concentrations, binding affinity and energy, and more importantly the flow velocity. For the current case, the simplest trial conditions were utilized for our model (Couette flow). Deviations from this ideal case can be investigated by future studies and potentially influence the parameters α and β in the derived model to account for turbulent flow, temperature effects, and viscosity, among other factors. Clearly, experimental analyses are needed to demonstrate the accuracy and reliability in the real world. Thus, experimental validation is an ongoing work in tandem with sensor development (Zhang et al. 2015a, b), which will be the subject of a future publication. Scaled collision theory reveals great potential to be used as a system design tool for a broad range of sensing applications, such as water, air, and food quality monitoring, biomedical detection, and point-of-care diagnostics.

Acknowledgments

W.Z., S.N., M.W., and S.W.C. acknowledge funding from Northeastern University's (NEU's) FY15 TIER 1 Interdisciplinary Research Seed Grant. S.W.C. acknowledges generous support from NEU's Civil and Environmental Engineering (CEE) Department. The calculations and the analysis were carried out using a parallel Linux cluster at NEU's Laboratory for Nanotechnology In Civil Engineering (NICE). Visualization has been carried out using the VMD visualization package.

Supplemental Data

Eq. (S1) and Figs. S1 and S2 are available online in the ASCE Library (www.ascelibrary.org).

References

Bialik, R. J. 2011. "Particle–particle collision in Lagrangian modelling of saltating grains." *J. Hydraul. Res.* 49 (1): 23–31. https://doi.org/10.1080/00221686.2010.543778.

Cao, J., J. Seegmiller, N. Q. Hanson, C. Zaun, and D. N. Li. 2015. "A microfluidic multiplex proteomic immunoassay device for translational research." *Clin. Proteom.* 12 (1): 28. https://doi.org/10.1186/s12014-015-9101-x.

Cate, D. M., J. A. Adkins, J. Mettakoonpitak, and C. S. Henry. 2015. "Recent developments in paper-based microfluidic devices." *Anal. Chem.* 87 (1): 19–41. https://doi.org/10.1021/ac503968p.

Chu, C. H., W. H. Chang, W. J. Kao, C. L. Lin, K. W. Chang, Y. L. Wang, and G. B. Lee. 2015. "An integrated microfluidic system with field-effect-transistor-based biosensors for automatic highly-sensitive C-reactive protein measurement." In *Proc., 28th IEEE Int. Conf. on Micro Electro Mechanical Systems (MEMS)*, 581–584. New York: IEEE.

Dawoud, A. A., T. Kawaguchi, and R. Jankowiak. 2007. "In-channel modification of electrochemical detector for the detection of bio-targets on microchip." *Electrochem. Commun.* 9 (7): 1536–1541. https://doi.org/10.1016/j.elecom.2007.02.016.

Dixit, C. K., and A. Kaushik. 2012. "Nano-structured arrays for multiplex analyses and lab-on-a-chip applications." *Biochem. Biophys. Res. Commun.* 419 (2): 316–320. https://doi.org/10.1016/j.bbrc.2012.02.018.

Engel, Y., R. Elnathan, A. Pevzner, G. Davidi, E. Flaxer, and F. Patolsky. 2010. "Supersensitive detection of explosives by silicon nanowire arrays." *Angewandte Chemie Int. Ed.* 49 (38): 6830–6835. https://doi.org/10.1002/anie.201000847.

Gompper, G., T. Ihle, D. M. Kroll, and R. G. Winkler. 2009. "Multi-particle collision dynamics: A particle-based mesoscale simulation approach to the hydrodynamics of complex fluids." Vol. 221 of *Advanced computer simulation approaches for soft matter sciences III. Advances in polymer science*, edited by C. Holm and K. Kremer, 1–87. Berlin, Heidelberg: Springer.

Gowers, S. A. N., V. F. Curto, C. A. Seneci, C. Wang, S. Anastasova, P. Vadgama, G. Z. Yang, and M. G. Boutelle. 2015. "3D printed microfluidic device with integrated biosensors for online analysis of subcutaneous human microdialysate." *Anal. Chem.* 87 (15): 7763–7770. https://doi.org/10.1021/acs.analchem.5b01353.

IUPAC (International Union of Pure and Applied Chemistry). 1997. *Compendium of chemical terminology*. 2nd ed. Oxford, UK: Blackwell Scientific Publications.

Jung, W., A. Jang, P. L. Bishop, and C. H. Ahn. 2011. "A polymer lab chip sensor with microfabricated planar silver electrode for continuous and on-site heavy metal measurement." *Sensors Actuators B.* 155 (1): 145–153. https://doi.org/10.1016/j.snb.2010.11.039.

Kapral, R. 2008. "Multiparticle collision dynamics: Simulation of complex systems on mesoscales." Vol. 140 of *Advances in chemal physics*, edited by S. A. Rice, 89–146. New York: Wiley.

Ko, Y. J., J. H. Maeng, Y. Ahn, S. Y. Hwang, N. G. Cho, and S. H. Lee. 2008. "Microchip-based multiplex electro-immunosensing system for the detection of cancer biomarkers." *Electrophoresis* 29 (16): 3466–3476. https://doi.org/10.1002/elps.200800139.

Kumar, S., S. Kumar, M. A. Ali, P. Anand, V. V. Agrawal, R. John, S. Maji, and B. D. Malhotra. 2013. "Microfluidic-integrated biosensors: Prospects for point-of-care diagnostics." *Biotechnol. J.* 8 (11): 1267–1279. https://doi.org/10.1002/biot.201200386.

Lee, J. U., A. H. Nguyen, and S. J. Sim. 2015. "A nanoplasmonic biosensor for label-free multiplex detection of cancer biomarkers." *Biosens. Bioelectron.* 74: 341–346. https://doi.org/10.1016/j.bios.2015.06.059.

Lefevre, F., A. Chalifour, L. Yu, V. Chodavarapu, P. Juneau, and R. Izquierdo. 2012. "Algal fluorescence sensor integrated into a microfluidic chip for water pollutant detection." *Lab Chip.* 12 (4): 787–793. https://doi.org/10.1039/C2LC20998E.

Lewis, W. 1918. *A system of physical chemistry*. London: Longmans, Green and Co.

Lisowski, P., and P. K. Zarzycki. 2013. "Microfluidic paper-based analytical devices (μPADs) and micro total analysis systems (μTAS): Development, applications and future trends." *Chromatographia* 76 (19–20): 1201–1214. https://doi.org/10.1007/s10337-013-2413-y.

Mark, D., S. Haeberle, G. Roth, F. von Stetten, and R. Zengerle. 2010. "Microfluidic lab-on-a-chip platforms: Requirements, characteristics and applications." *Chem. Soc. Rev.* 39 (3): 1153–1182. https://doi.org/10.1039/b820557b.

Marle, L., and G. M. Greenway. 2005. "Microfluidic devices for environmental monitoring." *Trac-Trend Anal. Chem.* 24 (9): 795–802. https://doi.org/10.1016/j.trac.2005.08.003.

Meredith, N. A., C. Quinn, D. M. Cate, T. H. Reilly, J. Volckens, and C. S. Henry. 2016. "Paper-based analytical devices for environmental analysis." *Analyst* 141 (6): 1874–1887. https://doi.org/10.1039/C5AN02572A.

Padding, J. T., and W. J. Briels. 2002. "Time and length scales of polymer melts studied by coarse-grained molecular dynamics simulations." *J. Chem. Phys.* 117 (2): 925–943. https://doi.org/10.1063/1.1481859.

Peters, K. L., I. Corbin, L. M. Kaufman, K. Zreibe, L. Blanes, and B. R. McCord. 2015. "Simultaneous colorimetric detection of improvised explosive compounds using microfluidic paper-based analytical devices (μPADs)." *Anal. Methods.* 7 (1): 63–70. https://doi.org/10.1039/C4AY01677G.

Plimpton, S. 1995. "Fast parallel algorithms for short-range molecular dynamics." *J. Comput. Phys.* 117 (1): 1–19. https://doi.org/10.1006/jcph.1995.1039.

Schlichting, H. 1955. *Boundary layer theory.* New York: McGraw-Hill.

Trautz, M. 1916. "Das Gesetz der Reaktionsgeschwindigkeit und der Gleichgewichte in Gasen. Bestätigung der Additivität von Cv-3/2R. Neue Bestimmung der Integrationskonstanten und der Moleküldurchmesser." *Zeitschrift für anorganische und allgemeine Chemie* 96 (1): 1–28. https://doi.org/10.1002/zaac.19160960102.

Wiener, N. 1921. "The average of an analytic functional and the Brownian movement." *Proc. Natl. Acad. Sci. U.S.A.* 7 (10): 294–298. https://doi.org/10.1073/pnas.7.10.294.

Yeo, L. Y., H. C. Chang, P. P. Y. Chan, and J. R. Friend. 2011. "Microfluidic devices for bioapplications." *Small* 7 (1): 12–48. https://doi.org/10.1002/smll.201000946.

Zhang, W., Y. Du, and M. L. Wang. 2015a. "Noninvasive glucose monitoring using saliva nano-biosensor." *Sens. Bio-Sens. Res.* 4: 23–29. https://doi.org/10.1016/j.sbsr.2015.02.002.

Zhang, W., Y. Du, and M. L. Wang. 2015b. "On-chip highly sensitive saliva glucose sensing using multilayer films composed of single-walled carbon nanotubes, gold nanoparticles, and glucose oxidase." *Sens. Bio-Sens. Res.* 4: 96–102. https://doi.org/10.1016/j.sbsr.2015.04.006.

Zhang, W., M. L. Wang, S. Khalili, and S. W. Cranford. 2016. "Materiomics for oral disease diagnostics and personal health monitoring: Designer biomaterials for the next generation biomarkers." *Omics J. Integr. Biol.* 20 (1): 12–29. https://doi.org/10.1089/omi.2015.0144.

Zhao, X. Y., and T. Dong. 2013. "A microfluidic device for continuous sensing of systemic acute toxicants in drinking water." *Int. J. Environ. Res. Pub. Health* 10 (12): 6748–6763. https://doi.org/10.3390/ijerph10126748.

Zhou, Q., D. Patel, T. Kwa, A. Haque, Z. Matharu, G. Stybayeva, Y. D. Gao, A. M. Diehl, and A. Revzin. 2015. "Liver injury-on-a-chip: Microfluidic co-cultures with integrated biosensors for monitoring liver cell signaling during injury." *Lab Chip* 15 (23): 4467–4478. https://doi.org/10.1039/C5LC00874C.